HHS Public Access

Author manuscript

IEEE Access. Author manuscript; available in PMC 2022 May 19.

Published in final edited form as:

IEEE Access. 2022 ; 10: 25062–25072. doi:10.1109/access.2022.3154824.

Characterization of a Low-Profile, Flexible, and Acoustically Transparent Receive-Only MRI Coil Array for High Sensitivity MR-Guided Focused Ultrasound

ISABELLE SANIOUR[1], **FRASER J. L. ROBB**[2] **[Member, IEEE]**, **VICTOR TARACILA**[2], **VISHWAS MISHRA**[1], **JANA VINCENT**[2] **[Member, IEEE]**, **HENNING U. VOSS**[1], **MICHAEL G. KAPLITT**[3], **J. LEVI CHAZEN**[1], **SIMONE ANGELA WINKLER**[1] **[Senior Member, IEEE]**

[1]Department of Radiology, Weill Cornell Medicine, NewYork-Presbyterian Hospital, New York, NY 10065, USA

[2]MR Engineering, GE Healthcare Coils, Aurora, OH 44202, USA

[3]Department of Neurological Surgery, Weill Cornell Medicine, NewYork-Presbyterian Hospital, New York, NY 10065, USA

Abstract

Magnetic resonance guided focused ultrasound (MRgFUS) is a non-invasive therapeutic modality for neurodegenerative diseases that employs real-time imaging and thermometry monitoring of targeted regions. MRI is used in guidance of ultrasound treatment; however, the MR image quality in current clinical applications is poor when using the vendor built-in body coil. We present an 8-channel, ultra-thin, flexible, and acoustically transparent receive-only head coil design (FUS-Flex) to improve the signal-to-noise ratio (SNR) and thus the quality of MR images during MRgFUS procedures. Acoustic simulations/experiments exhibit transparency of the FUS-Flex coil as high as 97% at 650 kHz. Electromagnetic simulations show a SNR increase of 13× over the body coil. In vivo results show an increase of the SNR over the body coil by a factor of 7.3 with 2× acceleration (equivalent to 11× without acceleration) in the brain of a healthy volunteer, which agrees well with simulation. These preliminary results show that the use of a FUS-Flex coil in MRgFUS surgery can increase MR image quality, which could yield improved focal precision, real-time intraprocedural anatomical imaging, and real-time 3D thermometry mapping.

INDEX TERMS

Magnetic resonance imaging; coils; ultrasonic transducer arrays

Corresponding author: Simone Angela Winkler (ssw4001@med.cornell.edu).

This work involved human subjects or animals in its research. Approval of all ethical and experimental procedures and protocols was granted by the Institutional Review Board (IRB) under Protocol No. 20–03021574.

I. INTRODUCTION

Magnetic resonance guided focused ultrasound (MRgFUS) has emerged as a non-invasive treatment modality in a number of applications, such as essential tremor [1]–[3], Parkinson's disease [4]–[6], neuropathy [7], [8], epilepsy [9], blood-brain barrier opening [10]–[13], and Alzheimer's disease [14]–[16].

MRgFUS systems use helmet-shaped transceivers with a large number of ultrasound (US) transducers (for instance, the INSIGHTEC ExAblate system comprises 1024 transducers) concentrating acoustic energy on a millimetric-sized focal point in the brain. In order to efficiently couple acoustic energy, a degassed water bath is placed between the ultrasound transducer and the skull. This water bath also serves as a cooling mechanism. The frequency and intensity of the acoustic energy can vary (220 kHz - 720 kHz) depending on the application.

To localize the sonication target, structural MRI is used [17], [18]. MR thermometry [19]–[22] is employed to monitor temperature/energy delivery in the target and healthy tissue during intervention. Furthermore, diffusion tensor imaging (DTI) aids the selection of ablation sites in preprocedural and intraprocedural planning [23].

However, poor imaging quality in many current MRgFUS exams precludes effective and fast image acquisition. First, a typical birdcage-like head receive coil cannot be used to achieve signal-to-noise-ratio (SNR) typically observed in MRI because the transducer does not leave adequate space. As a result, most MRgFUS techniques currently use the much larger and less efficient, vendor built-in, body-sized coil for both transmission and reception. Second, the high-permittivity water bath, together with the conductive transducer surface, causes significant B_1 inhomogeneities that produce the unwanted low-signal band artifacts [24] observed in MRgFUS images at the region of interest. This artifact tends to occur at the locations of the thalamus and hippocampus [25], [26], which are regions of interest for essential tremor and Alzheimer's disease.

Different receive coil arrays have been designed in order to achieve better SNR [20], [24], [27]–[33]. Bitton *et al.* proposed a 3T dual-channel receive coil integrated into the MRgFUS silicone sealant membrane [32]. The upper portion of the coil is submerged in the water bath, while the lower part sits outside, providing a SNR increase by a factor of 4 compared to the body coil. Watkins *et al.* proposed a volume coil design for 3T MRI that can be placed partially inside the water-filled transducer. This interior portion of the coil is inductively coupled to the portion of the coil that is located outside the transducer [28].

However, the evaluation of the acoustic footprint has not been tackled in great detail in MRgFUS related coil design, with the exception of the work of Corea *et al.*, in which the printed capacitor-based coil design exhibits experimentally evaluated, acoustic, shoot-through, transparency of up to 89.5% at 650 kHz and 80.5% at 1 MHz, allowing the coil to be placed in the acoustic path [30]. Phantom results show an increase in MRI SNR by a factor of 2 at the center of the phantom using a 4-channel printed receive coil.

In this paper, we aim to improve both imaging sensitivity and acoustic transparency in one apparatus by presenting a very thin, low-profile, receive-only 8-channel head coil (FUS-Flex) operating at 3T. The design is inspired by stretchable [34], [35], flexible [36]–[40] and lightweight [41] coil technologies, offering a coil array with full conformity to the head. The novelty of our work lies in the use of very thin (~1 mm) RF elements (providing low interaction with the acoustic field), and the use of higher channel count than currently available in the literature, increasing the available imaging SNR, the sensitivity of the coil and improving/enabling parallel imaging. Better receive SNR in the region of the low-signal band artifact can also indirectly reduce the associated sensitivity problems.

II. METHODS

A. COIL GEOMETRY

The proposed receive-only FUS-Flex coil consists of an 8-channel array using receive architecture inspired by highly flexible and thin coil technology [42], [43]. Each element has a diameter of 110 mm. The coil is designed to be placed conformally, and in a close-fitting fashion, around the circumference of the patient's head (Figure 1). The RF elements consist of a thin malleable conductor construction [36], [39], [42]–[46] comprising two parallel conductor wires encapsulated and separated by a dielectric material, the two parallel conductor wires maintained separate by the dielectric material along the entire length of the loop portion between terminating ends thereof (INCA, integrated distributed capacitors - thickness = 0.6 mm) with a poly-tetrafluoroethylene (PTFE) jacket (outer diameter ~1 mm) (GE Healthcare, Waukesha, WI, USA). The RF element is created from a flexible link resonator structure with the length of each resonator being no greater than 1/10th of the wavelength of the resonant RF field [47]. This design ensures tuning stability when loaded due to uniform charge distribution and internally confined irrotational electric fields within the resonator [48]. The smaller diameter size conductor lends itself to its application in MRgFUS due to substantially decreased acoustic scattering. The conductor, whose resistance measures 10 Ω with head loading, is attached to a feedboard utilizing a custom preamplifier with a noise figure of <0.5 dB, a gain of 28 dB at 127.7 MHz, and an input impedance of <3 Ω. Coil elements were placed with a fixed overlap of 30 mm in a 2D planar configuration. The effective preamplifier decoupling impedance is sufficiently robust (>1 kΩ) to facilitate element-to-element overlap beyond that of conventional critical coupling to accommodate the conforming of the array or different head sizes [44], [45]. The conservative electric field is strictly confined within the small cross-section of the two parallel wires and dielectric filler material. In the case of two RF coil loops overlapping, the parasitic capacitance at the cross-overs is greatly reduced in comparison to two overlapped copper traces of traditional RF coils. RF coil thin cross-sections allow better magnetic decoupling and reduce or eliminate critical overlap between two loops in comparison to two traditional trace-based coil loops [44], [45]. In the RF transmit phase a hybrid decoupling scheme is utilized [44].

The array is sewn on a quasi-acoustic transparent polyester fabric often used in loudspeaker designs (shown in blue in Figure 1B) (Guilford of Maine, ME, USA). The light weight of

the FUS-Flex coil and the breathability of the polyester fabric help improve patient comfort and allow patients to see and breathe normally during procedures.

B. ACOUSTIC SIMULATIONS AND EXPERIMENTS

The acoustic transparency of the FUS-Flex coil was evaluated by investigating the attenuation of the acoustic signal as well as the shift of the focal point in different coil placements using numerical simulation. To this goal, we studied the influence of the FUS-Flex coil material (conductor, dielectric, and fabric) on the acoustic focal point emitted by a 30 cm-diameter transducer. Case 1: the transducer was simulated without the RF coil present for reference (Figure 2A). Case 2: the 8-channel coil was placed around the focal point at a distance of 80 mm, mimicking the position of the coil around the patient's head (Figure 2B). Case 3: one RF element was placed directly in front of the acoustic source ("shoot-through") to study the acoustic transmission/attenuation directly through the coil and thus to quantify the attenuation from one coil element (Figure 2C). Simulations were performed using COMSOL Multiphysics® (COMSOL, Burlington, MA). Figure 2D, E show a model of a transducer (focal length 232 mm, radius 150 mm), water bath, and a cylindrically shaped tissue phantom to mimic the head (radius 150 mm, length 240 mm) [49], [50]. The thicknesses of the fabric, conductor, and coil dielectric were 1, 0.6, and 1 mm, respectively. The transducer was driven at typical low and high frequencies used in FUS treatment, i.e., 220 kHz and 650 kHz. For each case, the intensity magnitude, in W/m^2, was plotted along the z-coordinate through the focal point. The spatial resolution used in this simulation was approximately 0.01 mm.

The acoustic attenuation of the coil was also evaluated on the bench using 2 immersion transducers (500kHz, 00–011923_NF, Sensor Networks, Inc) in a container of water as shown in Figure 2F. The acoustic transmission attenuation was measured for the FUS-Flex coil and was compared to the INSIGHTEC membrane that was used to seal the 2-channel coil in the study by Bitton *et al.* [32]. This membrane is often used in MRgFUS settings when an acoustically transparent sealant material is required. We therefore included it in our acoustic tests as a known reference standard. The transducers were separated by 4.5 cm, and the material under test was positioned centrally between the two transducers.

C. ELECTROMAGNETIC SIMUALTIONS

We hypothesized that the proposed coil provides increased MR imaging SNR in (1) a non-MRgFUS exam compared to a conventional head coil (given its conformity and close proximity), and (2) in an MRgFUS exam in comparison to the vendor built-in body coil.

Numerical simulations were performed to analyze coil performance in both applications. SNR improvement was determined using the B_1^- field magnitude.

1) COMPARISION OF FUS-FLEX COIL TO CONVENTIONAL BIRDCAGE HEAD COIL—

After an MRgFUS procedure, a head coil is often used for a control scan without the transducer. Often the standard head birdcage is used. The conformal fit of the FUS-Flex coil could outperform the commercially available head coil even in a normal, non-MRgFUS exam as used at the end of an MRgFUS procedure and could also outperform a less

flexible phased array due to its increased distance from the skull. To investigate on this hypothesis, electromagnetic simulations of the 8-channel receive-only FUS-Flex array using an element diameter of 110 mm were performed using Sim4Life (Zurich MedTech, Zurich, Switzerland). Its performance was compared to a 16-leg conventional birdcage head coil (diameter: 300 mm; length: 200 mm), Figure 3A, B. For a realistic in silico scenario, a body model, Duke (IT'IS Foundation, Zurich, Switzerland), was used. The FUS-Flex coil array was considered to be of oval shape (semi-minor axis of 190 mm, semi-major axis of 216 mm). The conductors were chosen to be perfect electric conductors (PEC). Matching and tuning capacitors were used to tune the coil elements to 128 MHz and ensure a 50 Ω-match. Each RF element was driven by a 1V gaussian excitation signal with sequential phase increments of 45 degrees. In order to provide an estimation of the SNR with the receive-only FUS-Flex coil, we plotted the rotational component of the magnetic field B_1^-.

2) FUS-FLEX COIL WITHIN ULTRASOUND TRANSDUCER AND COMPARISION TO BODY COIL—

First, we replicated the low-signal bands that stem from the influence of the transducer on the transmit field by modeling an MRgFUS transducer of 30 cm diameter using a semispherical water-filled copper-coated geometry, placed over Duke's head (Figure 3C, E). We then evaluated the receive SNR of the proposed FUS-Flex coil and compared it to the commonly used 16-leg body coil (diameter: 620 mm; length: 570 mm) in order to quantify imaging performance increases.

D. COIL CHARACTERIZATION ON THE BENCH

Each loop of the 8-channel coil was subsequently tested on the bench using a single-loop pickup coil and a network analyzer. The transmission coefficient (quantified by S_{21}) between the coil element connected to an industry test fixture (port 1) and a pickup loop (port 2) was measured. The fixture allows active decoupling through biasing of the diode and allows connection to DC power supply. The RF response was evaluated for each RF element separately and within the array. The feedboard including the preamplifier was included in the measurements.

E. IN VIVO MR IMAGING

We hypothesized improved imaging SNR and evaluated the imaging signal. As such, we validated the improvement of the SNR with and without the presence of the water-filled transducer at the thalamus region. A GE Healthcare Discovery MR750 system was used. In vivo MR images with the FUS-Flex receive coil were acquired with institutional review board approval (IRB protocol number 20–03021574) and informed consent on healthy volunteers without (setup 1) and with the transducer (setup 2). Images were compared with the body coil in receive mode. A water-filled transducer (INSIGHTEC ExAblate neuro) was placed around the head of the two volunteers using the INSIGHTEC sealant membrane. GE's T1 weighted volume imaging (3D Bravo) sequence (TE = 3 ms, TR = 7.4 ms, FA = 12° and Pixel bandwidth = 244.1 Hz/px) used. The FUS-Flex coil was used in receive-only mode and the body coil was used as an RF transmitter. SNR was determined according to the NEMA MS 1–2008 standards publication (R2014, R2020) [51].

Note the coil was placed outside the water bath in the in vivo experiment to ensure electrical safety in this first, unsealed, feasibility evaluation.

III. RESULTS

A. ACOUSTIC TRANSPARENCY

Figure 4A, F show 2D maps of the acoustic field pressure for low and high frequencies and the interaction of the acoustic field with the coil in cases 2 and 3. The acoustic field magnitude is shown in Figure 4B–E, G–J; results along the z- and r- direction were normalized to the case without a coil (reference). The results along the z-direction (parallel to the wave propagation direction) for case 2 exhibit an attenuation of the peak intensity at the focal point at $z = 221$ mm) by 16% and 11% for 220 kHz and 650 kHz, respectively, and the displacement of the focal point was around 1.59 mm and 0.11 mm at 220 kHz and 650 kHz, respectively. In the third case, minor signal fluctuations were observed (<5%) with a shift of the focal point by less than 0.39 mm for both frequencies. Focal point locations along the r-direction (in plane/perpendicular to the direction of the wave propagation) were less affected, a negligible shift was observed at $r = 0$ mm), and the highest attenuation was observed for case 2: about 6% and 3% for the 220 kHz and 650 kHz frequencies, respectively.

The experimental measurements show that the relative acoustic attenuation (normalized to the case without a coil) due to the single-channel FUS-Flex coil varies from about 1% to 5% in the frequency range from 100 kHz to 700 kHz (Figure 5), which confirms the simulated results (case 3). The acoustic attenuation due the INSIGHTEC membrane varies from about 10% to 30% in the frequency range from 100 kHz to 700 kHz. In summary, the FUS-Flex coil outperforms the INSIGHTEC sealing membrane, which is specifically made to be acoustically transparent by the vendor.

B. ELECTROMAGNETIC SIMUALTIONS

1) COMPARISION OF FUS-FLEX COIL TO CONVENTIONAL BIRDCAGE HEAD COIL—

The use of the FUS-Flex coil improves the simulated B_1^- values, and therefore the SNR by a factor of 4× in the sagittal plane and 9× in the coronal plane over a standard birdcage head coil in the thalamus region (Figures 6A, B), demonstrating significantly improved performance even in a non-MRgFUS brain exam.

2) FUS-FLEX COIL WITHIN ULTRASOUND TRANSDUCER AND COMPARISION TO BODY COIL—

The RF signal reflection from the copper-coated transducer produces E-field minima and causes a typical low-signal band in MRgFUS images along with a significant reduction in B_1 magnitude (Figure 6).

Figures 6C, D show the simulated B_1^- maps for FUS-Flex and body coils, denoting a SNR improvement at the position of the thalamus of ~13× and ~15× with and without the transducer, respectively, in both sagittal and coronal planes.

C. COIL CHARACTERIZATION ON THE BENCH

We confirmed that the magnetic coupling between the coil elements was minimized through overlapping (Figure 7). The measured quality factor ratio ($Q_{unloaded}/Q_{loaded}$) was approximately 4.5 [46], [52], indicating sample dominant losses.

D. IN VIVO MR IMAGING

Images acquired using the FUS-Flex coil in Figure 8 depict the position of the thalamus in a healthy volunteer with high sensitivity and show clear improvement of the low-signal band. At this location, the SNR gain is 7.3-fold and 7.6-fold compared to the body coil, with and without the MRgFUS transducer present, respectively. Note that for a 2-fold acquisition time (t_{acq}), the experimental SNR increase factor (7.3 and 7.6) can be multiplied by √2 and equal ~11, which agrees with the simulation results.

We would also like to note that the position and intensity of the low-signal band artifact is the result of complex electromagnetic field interferences and reflections and strongly depends on a number of parameters, such as the positioning of the head, the amount of water used, and other factors. Since the volunteer in Figure 8 was not part of an actual MRgFUS surgical treatment, we did not use the typical mounting screws and frame for reasons of volunteer comfort. The head is slightly tilted and located off-center, resulting in a shift of the low-signal band to the frontal upper region of the brain, partially extending into the water bath. Overall, the simulated increase in SNR is a close match to the in vivo results for both volunteers, confirming the potential of FUS-Flex technology to yield improved MRgFUS imaging quality.

IV. DISCUSSION

In the above, we proposed the FUS-Flex concept, a new acoustically transparent 8-channel coil geometry, for use in MRgFUS neurosurgery. This is the first 8-channel coil built for transcranial MRgFUS applications. Choosing a coil array of 8 channels or more allows to not only increase the quality of the image, but to accelerate acquisition to provide fast, high-resolution imaging with accurate detection of the region of interest (ROI) and temperature monitoring, especially when parallel imaging is used. Increasing the number of channels can be easily achieved using coil technology with the heavy overlapping characteristic of RF elements beyond that of critical coupling [44], [45]. Current procedures often involve the coarse localization of the thalamus using the poor MR signal from the body coil. Non-ablative temperatures are then used to produce reversible sonication observable in the awake subject, thus providing a means to fine-tune the focal point at sub-millimetric accuracy. Our proposed coil array may avoid this tedious, risky, and uncomfortable calibration by providing suitable SNR and thus improved spatial resolution, directly usable to precisely locate the target region.

Current T2-weighted intraprocedural imaging can require a scan time of 3 min [2], [23] and is carried out late in the protocol when cooling time already requires a halt of the procedure. Allowing for acquisition times <1min could benefit real-time intraprocedural imaging and hence confirmation of energy delivery and measurement of the ablation site. Moreover,

diagnostic intraprocedural imaging could be useful when considering timing to conclude the treatment. Allowing 3D thermometry maps in real time, combined with active fusion to the DTI imaging, could help overcome the limitation of the body coil and improve the intraprocedural imaging utility.

Due to the severely degraded imaging performance, patients are often imaged without the transducer, using a standard birdcage head coil, after their treatment to obtain a high-resolution image of the target region. With the proposed FUS-Flex concept, it becomes attainable to provide such images at any time during the exam, interprocedurally, at a resolution that is potentially even higher than that of the birdcage head coil due to its decreased distance to the anatomy.

Highly flexible RF coil arrays are an emerging field of research even in applications that do not use MRgFUS. The fact that the coil array can be situated as conformally and as closely as possible with respect to the skin/skull (while obeying safety limits) maximizes the received MR signal and therefore the SNR in the MR image. Our proposed coil array is lightweight and flexible, allowing significant bending without performance decrease from geometry-dependent decoupling and resonance shifts that are normally observed in warped/stretched coil array designs [42].

It is to be noted that the FUS-Flex surface receive coil will not directly/completely solve the low-signal band artifact. While the FUS-Flex concept is a receive-only solution, the coil is located directly around the area of the brain with the infamous low-signal band, thus increasing SNR in the affected region (Figure 6C). Its increased receive SNR suggests feasibility to produce a significant increase of MRgFUS image quality over the body coil.

A large hindrance to the success of specific coil designs for MRgFUS has been their acoustic footprint and thus the distortion of ultrasound signal, which ultimately results in a physical shift, signal loss, and/or broadening of the focal point. The presented RF coil array is comprised of ultra-thin wiring mounted on acoustically transparent fabric. We simulated the presence of the FUS-Flex coil in an MRgFUS system using COMSOL Multiphysics and demonstrated the transparency of the coil when it is placed in the acoustic path. Our results indicate that the acoustic footprint of the coil is very small compared to the attenuation/aberration caused by the skull (70% of skull attenuation [53] versus 3% (650kHz) and 5% (220kHz) (shoot-through) as well as 11% (650kHz) and 16% (220kHz) (coil array around the head) of attenuation from our coil). Note that while lower frequencies are generally attenuated to a lower degree than their higher counterparts, they also propagate deeper into the tissue, potentially causing a larger scattered field and therefore a more pronounced interaction with the focal point. These findings are in line with Fig. 3a in [30]. In comparison, Köhler *et al.* showed that using a thin rod (Ø = 0.5 mm) placed in the path of the acoustic beam (shoot-through) decreases the acoustic pressure by only 1.6%, which means that the focal spot remains unaffected [54]. These results are consistent with those of the FUS-Flex coil presented here and demonstrate the importance of using thin wire coils in MRgFUS procedures. Moreover, the attenuation incurred here is reduced compared to the screen-printed design in [30]. In addition, the transducer elements can be selectively deactivated thus avoiding interaction with the coil elements. As a result, we do not expect

a major need to refocus the acoustic target location beyond what is already employed when correcting for the skull. The possibility to take into account the coil in the correction of the phase aberration, in a similar way to the skull, will be studied to further improve the acoustic attenuations.

Our final clinical goal for this work is to use the coil entirely (or sometimes partially, depending on anatomy) inside the water bath. At this proof-of-concept stage, we do not yet incorporate a fully sealed, waterproof, design. Inserting the coil into the water bath requires additional work with regard to transparency, air bubbles, and water permeability. Electrical safety is a big concern when working with in vivo subjects as well as costly MRI systems. This is outside the scope of this feasibility study and part of current and future work. Yet, we show that even with this low-profile 8-channel coil placed outside the water bath, we improve SNR significantly. The acoustic evaluation (experiment/simulation) along with the RF investigation (simulation partially/fully inside water bath, experiment outside water bath) performed in this paper suggest feasibility of full immersion once practical details of safe coil sealing are accomplished.

Future work will involve the use of higher channel counts to further increase the SNR and shorten acquisition time. A possible tradeoff between the number of channels and acoustic performance of the coil will be investigated. Along with increasing the number of channels, we can further optimize sequences to fall below the one-minute mark and thus allow for optimized intraprocedural acquisition. The FUS-coil can allow sequences such as DTI and 3D thermometry to achieve better results compared to the body coil in terms of image resolution and scan time and thus efficient monitoring of target and surrounding tissue. Future work will also include acoustic evaluation using the INSIGHTEC transducer as well as potential degassing of the coil fabric to remove air bubbles.

V. CONCLUSION

The proposed FUS-Flex coil is lightweight, stretchable, ultra-thin, and can potentially be adjusted to different head sizes and shapes without adding extra weight to the head while allowing the patient to see and breathe normally during procedures. When placing the FUS-Flex coil outside the water bath, the SNR is improved a factor of 7.3 with 2× acceleration (equivalent to 11× without acceleration), leading to a higher SNR efficiency. Acoustic simulations and experiments show a negligible influence of the coil on the position of the focal point and acoustic signal for deep target applications (98% transparency simulated/measured).

ACKNOWLEDGMENT

The authors would like to thank Dr. Scott Lindsay and Dr. Robert Stormont for inspiration and Muc Du and Jojo Borja of CBIC for helpful technical discussions and the valuable assistance of Cynthia Fox in the proofreading of the manuscript.

This work was supported by the National Institutes of Health under Grant NIH R00EB024341 and GE Healthcare.

Biographies

ISABELLE SANIOUR received the master's degree in sensors, measurement and instrumentation from Sorbonne University Pierre and Marie Curie Campus in partnership with ESPCI, Paris, France, in 2013, and the Ph.D. degree in biomedical physics from Claude Bernard University Lyon 1, in 2017. She worked on the design and development of a radio frequency MR coil with optical transmission of electrical signals and assessment of the RF electric field using an electro-optic probe. From 2018 to 2019, she was involved in research on superconducting radiofrequency coils with the University of Paris-Sud, Orsay, France. She is currently a Postdoctoral Associate with the Winkler Laboratory, Weill Cornell Medicine. Her research interests include the development of radiofrequency coils and hardware and the assessment of specific absorption rate for MR engineering applications.

FRASER J. L. ROBB (Member, IEEE) has been in the field of MRI hardware, starting his graduate school studies with the University of Aberdeen, since 1990, under Prof. David Lurie and Prof. James Hutchison. His Ph.D. thesis title was Field-Cycled Proton Electron Double Resonance Imaging of Dissolved Oxygen which gave him both wonderful hardware training and also an appreciation for physiology and metabolism. He learned to build MRI systems from basic components. Subsequently, he was a Research Assistant Professor in radiology with the Dartmouth College, New Hampshire, from 1997 to 1999, working for Prof. Harold Swartz on 1.1GHz ESR spectroscopic hardware. Most of his career has been heavily focused on commercial MRI coil design, starting with USA Instruments/GE Healthcare Inc., since 2000, and has more than 40 patents approved or in process on MRI coils. In recent year's, he has been pioneering advanced prototyping and simulation methods for MRI coils and developed the strategy which led to the air technology MRI coil revolution. He has been recognized internally as one of GE's most prolific inventors of recent times and led the strategy that led to the development of air coil technology and has an Honorary Professorship from the University of Sheffield, U.K.

VICTOR TARACILA received the B.S. and M.S. degrees in physics from the University of Bucharest and the Ph.D. degree in physics from Case Western Reserve University (CWRU), Cleveland, OH, USA. He is currently a Senior Architect at GE Healthcare Coils, Aurora, OH, USA. For over 15 year's, he works in MRI receive coil design, contributing with 40 patents. He is an Expert in FEM electromagnetic simulations of problems related to MRI receivers and transmitters. Occasionally, he teaches classes on MRI topics to students and fellow colleagues. He regularly coaches the M.S. and Ph.D. candidates on their research projects. He is an Active Member of International Society of Magnetic Resonance in Medicine (ISMRM), where he publishes and presents annually in society's main conferences.

VISHWAS MISHRA received the B.Tech. degree from the Indian Institute of Technology Guwahati, in 2020. He is currently pursuing the degree in physiology, biophysics and systems biology (PBSB) program with the Weill Cornell Graduate School. In the Winkler Laboratory, he is working on MR guided focused ultrasound coils and their implications in targeted tissue thermal ablation for treating neuropathic pain. His research interests include the field of computational neuroscience and systems biology.

JANA VINCENT (Member, IEEE) received the M.S. degree in electrical and computer engineering and the Ph.D. degree in biomedical engineering from Purdue University, West Lafayette, IN, USA, in 2021. From 2016 to 2019, she was a Teaching Assistant with the Weldon School of Biomedical Engineering, Purdue University, and the Department of Biological Sciences, where during this time, she was also a Research Assistant with the Magnetic Resonance Biomedical Engineering Laboratory. From 2020 to 2021, she was an Advanced Technology Coil Intern at GE Healthcare Coils, Aurora, OH, USA, where she has been a Senior MRI Coil Engineer, since 2021. She is currently working as the MR Engineering Study Group Trainee Representative. Her research interests include the development of magnetic resonance imaging hardware, including radiofrequency coils and cable traps. She is a member of the International Society for Magnetic Resonance in Medicine. She is also a member of the Biomedical Engineering Society (BMES) and Society of Women Engineers (SWE).

HENNING U. VOSS received the Ph.D. degree in physics from the University of Potsdam, Germany, in 1998. From 2000 to 2003, he was an Assistant Professor with the University of Freiburg, Germany, before becoming an Assistant Professor in physics in radiology with Weill Cornell Medical, New York City. He became an Associate Professor in physics in radiology, in 2009. At the beginning of 2021, he became the Technical Director of the Cornell Magnetic Resonance Imaging Facility (CMRIF) with the College of Human Ecology, Cornell University, Ithaca, NY, USA. His current research interests include new MRI imaging contrasts, MRI radiofrequency coils, dynamical systems, the application of dynamical systems methods to 4D (space and time) MRI data of the brain, and understanding of the aging human brain by using novel dynamical MRI contrasts to map aging-induced changes of the brain's physical properties, such as the elasticity of its arteries.

MICHAEL G. KAPLITT received the degree *(magna cum laude)* in molecular biology and Russian studies from Princeton University, in 1987, the Ph.D. degree in molecular neurobiology from The Rockefeller University, in 1993, and the M.D. degree from the Cornell Medical College, in 1995, both through Tri-Institutional M.D.-Ph.D. Program. Following his Neurosurgery Residency and a Chief Residency at Cornell, he completed a fellowship in stereotactic and functional neurosurgery with Dr. Andres Lozano with the University of Toronto, prior to joining our staff as an Assistant Professor in neurological surgery, in July 2001. His clinical activities focus upon using minimally invasive, stereotactic techniques for the treatment of functional disorders, such as Parkinson's disease, essential tremor and epilepsy. He also uses surgical methods to implant devices, such as spinal cord stimulators and opiate pumps to treat complex pain. He is also an Expert in the treatment of trigeminal neuralgia and hydrocephalus. He has pioneered the use of gene therapy in the brain. He has published over 40 papers and has edited two books on this subject. He recently completed the first clinical trial of gene therapy for Parkinson's disease for FDA approval, and his laboratory is actively researching mechanisms of cell death in diseases, such as Parkinson's and Huntington's. He was a recipient of numerous awards, including the Young Investigator Award from the American Society for Gene Therapy and he was named to Crain's 40 under 40 list for 2004.

J. LEVI CHAZEN received the B.S. degree (Hons.) in biomedical engineering from Johns Hopkins University, in 2002, and the M.D. degree *(magna cum laude)* from the Jefferson Medical College, Philadelphia, PA, USA, in 2007. He graduated top five in his class and was inducted into the Alpha Omega Alpha (AOA) Medical Honor Society. Following an internship in internal medicine, he completed a diagnostic radiology residency at NewYork-Presbyterian Hospital/Weill Cornell Medicine, from 2008 to 2012. He achieved board certification in diagnostic radiology from the American Board of Radiology, in July 2012. He went on to complete a neuroradiology fellowship with the University of California at San Francisco (UCSF) Medical Center. He joined the Weill Cornell Medicine Department, Radiology Faculty, in August 2013, where he worked as the Neuroradiology Fellowship Program Director and was promoted to an Associate Professor in radiology on a track recognizing clinical excellence, academic achievement, and innovation. He joined the HSS Faculty, in 2021, as the Director of Spine Imaging.

SIMONE ANGELA WINKLER (Senior Member, IEEE) received the degree in electrical engineering from the École Polytechnique Montréal, Canada, and the degree (Hons.) in mechatronics from Johannes Kepler University Linz, Austria. She specialized in RF/microwave engineering, funded by two fellowships (DOC fellowship/Austrian Academy of Science; first rank in the competition for a Ph.D. fellowship from FQRNT Québec) with the École Polytechnique Montréal. She is currently a Stanford-Trained NIH K99/R00 funded an Assistant Professor in radiology at Weill Cornell Medicine and leading expert in the ultra high-field (UHF) MRI community. Her research interests include the development of technology for the detection of subtle brain features for the diagnostics and monitoring of neurodegenerative and neuropsychiatric diseases, which ultimately provides a pathway to therapy through MR guidance. She was awarded with the first place in the MR Engineering Competition at the 2015 Annual Meeting of the ISMRM for a Thermoacoustic MRI Safety System and has earned a 2015, 2018, and 2021 Summa and Magna Cum Laude Merit Award for her oral presentations on RF coil designs, all of which are key components for ultra high-field MRI. Her research has appeared in over 60 journals, conferences, and patent submissions. She was also honored for her position as a lecturer in electromagnetic theory and has served on the editorial board of nine international journals and a scientific book publisher. For her research work during her M.Sc. and Ph.D. degrees, she has received numerous scientific awards and scholarships. During her postdoctoral work at McGill University, Montréal, Canada, she developed a microwave near-field imaging system for breast cancer detection. She committed to a postdoctoral fellow position at Stanford

University in ultra high-field MRI engineering (funded by a Canadian NSERC research fellowship, from 2012 to 2014), in 2012, where she became a Research Associate, in 2015.

REFERENCES

[1]. Elias WJ, Huss D, Voss T, and Loomba J, "A pilot study of focused ultrasound thalamotomy for essential tremor," New England J. Med, vol. 369, no. 7, pp. 640–648, Aug. 2013, doi: 10.1056/nejmoa1300962. [PubMed: 23944301]

[2]. Levi Chazen J, Stradford T, and Kaplitt MG, "Cranial MR-guided focused ultrasound for essential tremor," Clin. Neuroradiol, vol. 29, no. 2, pp. 351–357, Jun. 2019, doi: 10.1007/s00062-018-0709-x. [PubMed: 30046918]

[3]. Lipsman N, Schwartz ML, Huang Y, Lee L, and Sankar T, "MR-guided focused ultrasound thalamotomy for essential tremor: A proof-of-concept study," Lancet Neurol, vol. 12, no. 5, pp. 462–468, 2013, doi: 10.1016/s1474-4422(13)70048-6. [PubMed: 23523144]

[4]. Magara A, Buhler R, Moser D, Kowalski M, Pourtehrani P, and Jeanmonod D, "First experience with MR-guided focused ultrasound in the treatment of Parkinson's disease," J. Theory Ultrasound, vol. 2, p. 11, May 2014, doi: 10.1186/2050-5736-2-11.

[5]. Miller TR, Guo S, Melhem ER, and Eisenberg HM, "Predicting final lesion characteristics during MR-guided focused ultrasound pallidotomy for treatment of Parkinson's disease," J. Neurosurg, vol. 134, no. 5, pp. 1083–1090, 2020, doi: 10.3171/2020.2.jns192590. [PubMed: 32330882]

[6]. Fishman P and Lipsman N, "Focused ultrasound as an evolving therapy for Parkinson's disease," Movement Disorders, vol. 34, no. 9, pp. 1241–1242, Sep. 2019, doi: 10.1002/mds.27809. [PubMed: 31539464]

[7]. McClintic AM, Dickey TC, Gofeld M, Kliot M, Loeser JD, Richebe P, and Mourad PD, "Intense focused ultrasound preferentially stimulates subcutaneous and focal neuropathic tissue: Preliminary results," Pain Med, vol. 14, no. 1, pp. 84–92, Jan. 2013, doi: 10.1111/j.1526-4637.2012.01510.x. [PubMed: 23137045]

[8]. Jeanmonod D, Werner B, Morel A, and Michels L, "Transcranial magnetic resonance imaging–guided focused ultrasound: Noninvasive central lateral thalamotomy for chronic neuropathic pain," Neurosurgical Focus, vol. 32, no. 1, p. E1, 2012, doi: 10.3171/2011.10.focus11248.

[9]. Parker WE, Weidman EK, Chazen JL, and Niogi SN, "Magnetic resonance–guided focused ultrasound for ablation of mesial temporal epilepsy circuits: Modeling and theoretical feasibility of a novel noninvasive approach," J. Neurosurg, vol. 133, no. 1, pp. 63–70, 2020, doi: 10.3171/2019.4.jns182694.

[10]. Lipsman N, Meng Y, Bethune AJ, Huang Y, Lam B, Masellis M, Herrmann N, Heyn C, Aubert I, Boutet A, Smith GS, Hynynen K, and Black SE, "Blood–brain barrier opening in Alzheime's disease using MR-guided focused ultrasound," Nature Commun, vol. 9, no. 1, p. 2336, 2018, doi: 10.1038/s41467-018-04529-6. [PubMed: 30046032]

[11]. Abrahao A, Meng Y, Llinas M, Huang Y, Hamani C, Mainprize T, Aubert I, Heyn C, Black SE, Hynynen K, Lipsman N, and Zinman L, "First-in-human trial of blood–brain barrier opening in amyotrophic lateral sclerosis using MR-guided focused ultrasound," Nature Commun, vol. 10, no. 1, p. 4373, Sep. 2019, doi: 10.1038/s41467-019-12426-9. [PubMed: 31558719]

[12]. Mainprize T, Lipsman N, Huang Y, Meng Y, Bethune A, Ironside S, Heyn C, Alkins R, Trudeau M, Sahgal A, Perry J, and Hynynen K, "Blood-brain barrier opening in primary brain tumors with non-invasive MR-guided focused ultrasound: A clinical safety and feasibility study," Sci. Rep, vol. 9, no. 1, p. 321, Dec. 2019, doi: 10.1038/s41598-018-36340-0. [PubMed: 30674905]

[13]. Conti A, Kamimura HAS, Novell A, Duggento A, and Toschi N, "Magnetic resonance methods for focused ultrasound-induced blood-brain barrier opening," Frontiers Phys, vol. 8, p. 393, Sep. 2020, doi: 10.3389/fphy.2020.547674.

[14]. Beisteiner R, Matt E, Fan C, Baldysiak H, Schönfeld M, Novak TP, Amini A, Aslan T, Reinecke R, Lehrner J, and Weber A, "Transcranial pulse stimulation with ultrasound in Alzheimer's disease—A new navigated focal brain therapy," Adv. Sci, vol. 7, no. 3, 2020, Art. no. 1902583, doi: 10.1002/advs.201902583.

[15]. Bobola MS, Chen L, Ezeokeke CK, Olmstead TA, Nguyen C, Sahota A, Williams RG, and Mourad PD, "Transcranial focused ultrasound, pulsed at 40 Hz, activates microglia acutely and reduces Aβ load chronically, as demonstrated *in vivo*," Brain Stimulation, vol. 13, no. 4, pp. 1014–1023, 2020, doi: 10.1016/j.brs.2020.03.016. [PubMed: 32388044]

[16]. Nicodemus NE, Becerra S, Kuhn TP, Packham HR, Duncan J, Mahdavi K, Iovine J, Kesari S, Pereles S, Whitney M, Mamoun M, Franc D, Bystritsky A, and Jordan S, "Focused transcranial ultrasound for treatment of neurodegenerative dementia," Alzheimer's Dementia: Transl. Res. Clin. Interventions, vol. 5, no. 1, pp. 374–381, Jan. 2019, doi: 10.1016/j.trci.2019.06.007.

[17]. Ghanouni P, Pauly KB, Elias WJ, Henderson J, Sheehan J, Monteith S, and Wintermark M, "Transcranial MRI-guided focused ultrasound: A review of the technologic and neurologic applications," Amer. J. Roentgenol, vol. 205, no. 1, pp. 150–159, Jul. 2015, doi: 10.2214/AJR.14.13632. [PubMed: 26102394]

[18]. Jolesz FA, "MRI-guided focused ultrasound surgery," Annu. Rev. Med, vol. 60, no. 1, pp. 417–430, Feb. 2009, doi: 10.1146/annurev.med.60.041707.170303. [PubMed: 19630579]

[19]. Rieke V and Pauly KB, "MR thermometry," J. Magn. Reson. Imag, vol. 27, no. 2, pp. 376–390, Feb. 2008, doi: 10.1002/jmri.21265.

[20]. Odéen H, de Bever J, Almquist S, Farrer A, Todd N, Payne A, Snell JW, Christensen DA, and Parker DL, "Treatment envelope evaluation in transcranial magnetic resonance-guided focused ultrasound utilizing 3D MR thermometry," J. Therapeutic Ultrasound, vol. 2, no. 1, p. 19, 2014, doi: 10.1186/2050-5736-2-19.

[21]. Huang Y, Lipsman N, Schwartz ML, Krishna V, Sammartino F, Lozano AM, and Hynynen K, "Predicting lesion size by accumulated thermal dose in MR-guided focused ultrasound for essential tremor," Med. Phys, vol. 45, no. 10, pp. 4704–4710, Oct. 2018, doi: 10.1002/mp.13126. [PubMed: 30098027]

[22]. Rieke V, Vigen KK, Sommer G, Daniel BL, Pauly JM, and Butts K, "Referenceless PRF shift thermometry," Magn. Reson. Med, vol. 51, no. 6, pp. 1223–1231, Jun. 2004, doi: 10.1002/mrm.20090. [PubMed: 15170843]

[23]. Chazen JL, Sarva H, Stieg PE, Min RJ, Ballon DJ, Pryor KO, Riegelhaupt PM, and Kaplitt MG, "Clinical improvement associated with targeted interruption of the cerebellothalamic tract following MR-guided focused ultrasound for essential tremor," J. Neurosurg, vol. 129, no. 2, pp. 315–323, Aug. 2018, doi: 10.3171/2017.4.jns162803. [PubMed: 29053074]

[24]. Hadley JR, Odéen H, Merrill R, Adams SI, Rieke V, Payne A, and Parker DL, "Improving image quality in transcranial magnetic resonance guided focused ultrasound using a conductive screen," Magn. Reson. Imag, vol. 83, pp. 41–49, Nov. 2021, doi: 10.1016/j.mri.2021.07.002.

[25]. Yan X, Allen S, and Grissom WA, "'Propeller beanie' passive antennas to alleviate dark bands transcranial MR-guided focused ultrasound," in Proc. 28th Annu. Meeting ISMRM, 2020, p. 0113.

[26]. Yan X, Gore JC, and Grissom WA, "Traveling-wave meets standing-wave: A simulation study using pair-of-transverse-dipole-ring coils for adjustable longitudinal coverage in ultra-high field MRI," Concepts Magn. Reson. B, Magn. Reson. Eng, vol. 48B, no. 4, Oct. 2018, Art. no. e21402, doi: 10.1002/cmr.b.21402.

[27]. Gagliardo C, Midiri M, Cannella R, Napoli A, Wragg P, Collura G, Marrale M, Vincenzo Bartolotta T, Catalano C, and Lagalla R, "Transcranial magnetic resonance-guided focused ultrasound surgery at 1.5T: A technical note," Neuroradiol. J, vol. 32, no. 2, pp. 132–138, Apr. 2019, doi: 10.1177/1971400918818743. [PubMed: 30561246]

[28]. Watkins RD, Bitton R, and Butts Pauly K, "Integration of an inductive driven axially split quadrature volume coil with MRgFUS system for treatment of human brain," presented at the 22nd Annu. Meeting ISMRM, Milan, Italy, 2014.

[29]. Iacopino DG, Gagliardo C, and Giugno A, "Preliminary experience with a transcranial magnetic resonance–guided focused ultrasound surgery system integrated with a 1.5-T MRI unit in a series of patients with essential tremor and Parkinson's disease," Neurosurgical Focus, vol. 44, no. 2, p. E7, Feb. 2018, doi: 10.3171/2017.11.FOCUS17614.

[30]. Corea J, Ye P, Seo D, Butts-Pauly K, Arias AC, and Lustig M, "Printed receive coils with high acoustic transparency for magnetic resonance guided focused ultrasound," Sci. Rep, vol. 8, no. 1, pp. 1–10, Dec. 2018, doi: 10.1038/s41598-018-21687-1. [PubMed: 29311619]

[31]. Jones M, Hadley J, Minalga E, Snell J, and Hananel A, “Improving MR image quality for FUS treatments: Initial results from an ultrasound-compatible RF coil,” in Proc. Focused Ultrasound 3rd Int. Symp., Washington, DC, USA, 2012, p. 123.

[32]. Bitton RR, Sheingaouz E, Assif B, Kelm N, Dayan M, Butts Pauly K, and Ghanouni P, “Evaluation of an MRI receive head coil for use in transcranial MR guided focused ultrasound for functional neurosurgery,” Int. J. Hyperthermia, vol. 38, no. 1, pp. 22–29, Jan. 2021, doi: 10.1080/02656736.2020.1867242. [PubMed: 33459092]

[33]. Odéen H, de Bever J, Almquist S, Farrer A, Todd N, Payne A, Snell JW, Christensen DA, and Parker DL, “Treatment envelope evaluation in transcranial magnetic resonance-guided focused ultrasound utilizing 3D MR thermometry,” J. Therapeutic Ultrasound, vol. 2, no. 1, p. 19, 2014, doi: 10.1186/2050-5736-2-19.

[34]. Nordmeyer-Massner JA, De Zanche N, and Pruessmann KP, “Stretchable coil arrays: Application to knee imaging under varying flexion angles,” Magn. Reson. Med, vol. 67, no. 3, pp. 872–879, 2012, doi: 10.1002/mrm.23240. [PubMed: 22213018]

[35]. Motovilova E, Tan ET, Taracila V, Vincent JM, Grafendorfer T, Shin J, Potter HG, Robb FJL, Sneag DB, and Winkler SA, “Stretchable self-tuning MRI receive coils based on liquid metal technology (LiquiTune),” Sci. Rep, vol. 11, no. 1, Dec. 2021, doi: 10.1038/s41598-021-95335-6.

[36]. Cogswell PM, Trzasko JD, and Gray EM, “Application of adaptive image receive coil technology for whole-brain imaging,” Amer. J. Roentgenol, vol. 216, no. 2, pp. 552–559, Feb. 2021, doi: 10.2214/AJR.20.22812. [PubMed: 33236945]

[37]. Saniour I, Robb F, Taracila V, Vincent J, and Voss HH, “Acoustically transparent and low-profile head coil for high precision magnetic resonance guided focused ultrasound at 3T,” in Proc. 29th Annu. Meeting ISMRM, 2021, p. 4263.

[38]. Saniour I, Fraser R, Taracila V, Voss HH, and Kaplitt MG, “Attenuation of the dark band artifact in MR-guided focused ultrasound using an ultra-flexible high-sensitivity head coil,” in Proc. 29th Annu. Meeting ISMRM, 2021, p. 4010.

[39]. Stickle Y-J, “A novel ultra-flexible high-resolution AIR (Adaptive imaging receive) 64-channel bilateral phased array for 3T brachial plexus MRI,” in Proc. Int. Soc. Mag. Reson. Med, 2020, p. 4025.

[40]. Gruber B, Rehner R, Laistler E, and Zink S, “Anatomically adaptive coils for MRI—A 6-channel array for knee imaging at 1.5 Tesla,” Frontiers Phys, vol. 8, p. 80, Apr. 2020, doi: 10.3389/fphy.2020.00080.

[41]. Winkler SA, Corea J, Lechêne B, and O’Brien K, “Evaluation of a flexible 12-channel screen-printed pediatric MRI coil,” Radiology, vol. 291, no. 1, pp. 180–185, 2019, doi: 10.1148/radiol.2019181883. [PubMed: 30806599]

[42]. McGee KP, Stormont RS, and Lindsay SA, “Characterization and evaluation of a flexible MRI receive coil array for radiation therapy MR treatment planning using highly decoupled RF circuits,” Phys. Med. Biol, vol. 63, no. 8, 2018, Art. no. 08NT02, doi: 10.1088/1361-6560/aab691.

[43]. Collick BD, Behzadnezhad B, and Hurley SA, “Rapid development of application-specific flexible MRI receive coils,” Phys. Med. Biol, vol. 65, no. 19, 2020, Art. no. 19NT01, doi: 10.1088/1361-6560/abaffb.

[44]. Stormont RS, Lindsay SA, Taracila V, Mustafa G, Malik NM, Robb FJL, and Chu D, “Systems for a radio frequency coil for MR imaging,” U.S. Patent 16 463 575, Nov. 22, 2019. [Online]. Available: https://patents.google.com/patent/US20190277926A1/en

[45]. Stack C, Grafendorfer T, Robb F, and Falk S, “Flexible radio frequency coil array with detachable straps for MR imaging,” U.S. Patent 16 196 558, Nov. 11, 2019. [Online]. Available: https://patents.google.com/patent/US20190154775A1/en?oq=US20190154775A1

[46]. Vasanawala SS, Stormont R, Lindsay S, and Grafendorfer T, “Development and clinical implementation of very light weight and highly flexible AIR technology arrays,” in Proc. 25th Annu. Meeting ISMRM, 2017, p. 0755.

[47]. Veenstra H and Long JR, Circuit and Interconnect Design for RF and High Bit-rate Applications (Analog Circuits and Signal Processing). Amsterdam, The Netherlands: Springer, 2008.

[48]. Sutherland J. (1999). AS Edge Speeds Increase, Wires Become Transmission Lines. [Online]. Available: https://m.eet.com/media/1140649/19791-85208.pdf

[49]. Clavet T, "Using simulation to study ultrasound focusing for clinical applications," in COMSOL Multiphysics. 2017. [Online]. Available: https://www.comsol.com/blogs/using-simulation-to-study-ultrasound-focusing-for-clinical-applications/

[50]. Winkler SA, Alejski A, Wade T, McKenzie CA, and Rutt BK, "On the accurate analysis of vibroacoustics in head insert gradient coils," Magn. Reson. Med, vol. 78, no. 4, pp. 1635–1645, Oct. 2017, doi: 10.1002/mrm.26543. [PubMed: 27859549]

[51]. Determination of Signal-to-Noise Ratio (SNR) in Diagnostic Magnetic Resonance Imaging, N. E. M. Association, Rosslyn, Arlington, VA, USA, 2021.

[52]. Gruber B, Froeling M, Leiner T, and Klomp DWJ, "RF coils: A practical guide for nonphysicists," J. Magn. Reson. Imag, vol. 48, no. 3, pp. 590–604, Sep. 2018, doi: 10.1002/jmri.26187.

[53]. Pinton G, Aubry J-F, Bossy E, Müller M, Pernot M, and Tanter M, "Attenuation, scattering, and absorption of ultrasound in the skull bone," Med. Phys, vol. 39, pp. 299–307, Jan. 2012, doi: 10.1118/1.3668316. [PubMed: 22225300]

[54]. Köhler MO, Tillander M, Syrjä A, Nakari R, and Ylihautala M, "Ultrasound-transparent RF coil design for improved MR thermometry of HIFU therapy," in Proc. 19th Annu. Meeting ISMRM, 2011, p. 1728.

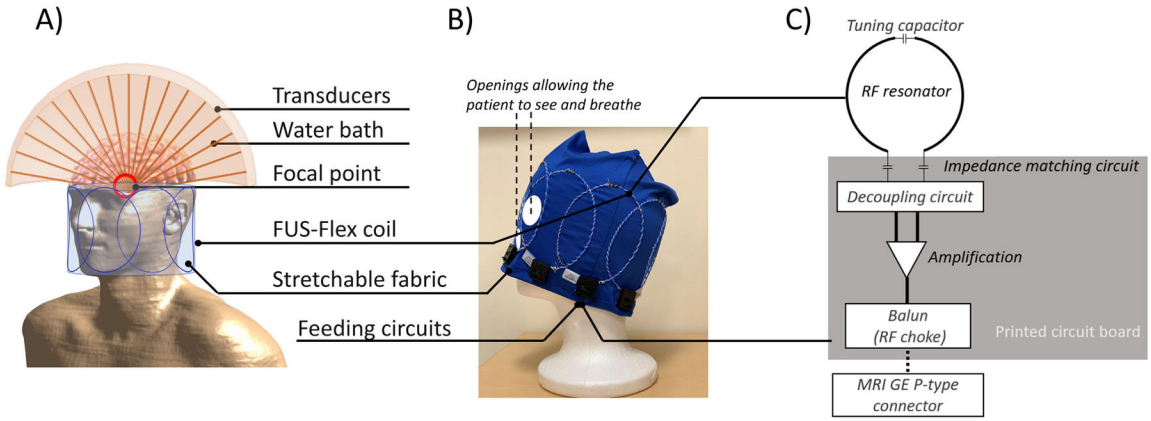

FIGURE 1.

A) Drawing showing the FUS-Flex coil and transducer placed around a human head model. B) Photograph of the 8-channel FUS-Flex coil. C) Schematic of one RF resonator along with the main components of the feeding circuit.

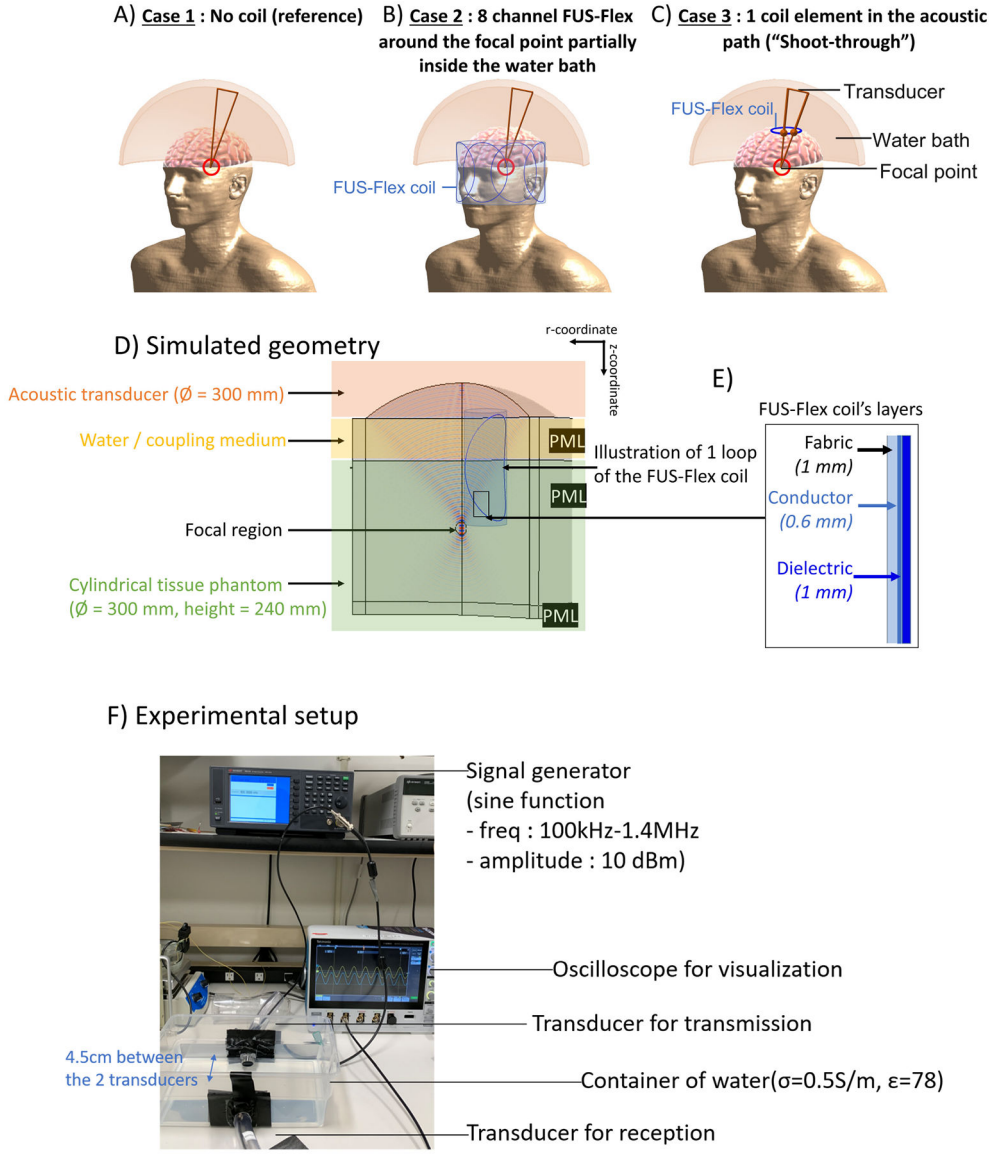

FIGURE 2.

Illustration of the transducer A) without a coil (case 1); B) with an 8-channel FUS-Flex coil placed around the focal point (case 2); and C) 1 channel FUS-Flex coil "shoot-through" (case 3). The 3 cases were simulated using a cylindrical phantom to mimic tissue. D) 3D simulation model with cylindrical phantom. The 30cm transducer is represented by the top dome in orange. The cylindrical phantom used is shown in green. The black lines at the exterior of the phantom/water represent perfectly matched layers used to absorb outgoing waves. Different orientations/positions of the coil (blue line, shown enlarged for better illustration, not to scale) were simulated as illustrated in Figure 2A–C. E) A magnified view of the different layers of the FUS-Flex coil. F) Experimental bench setup to measure the acoustic attenuation incurred due to the FUS-Flex coil.

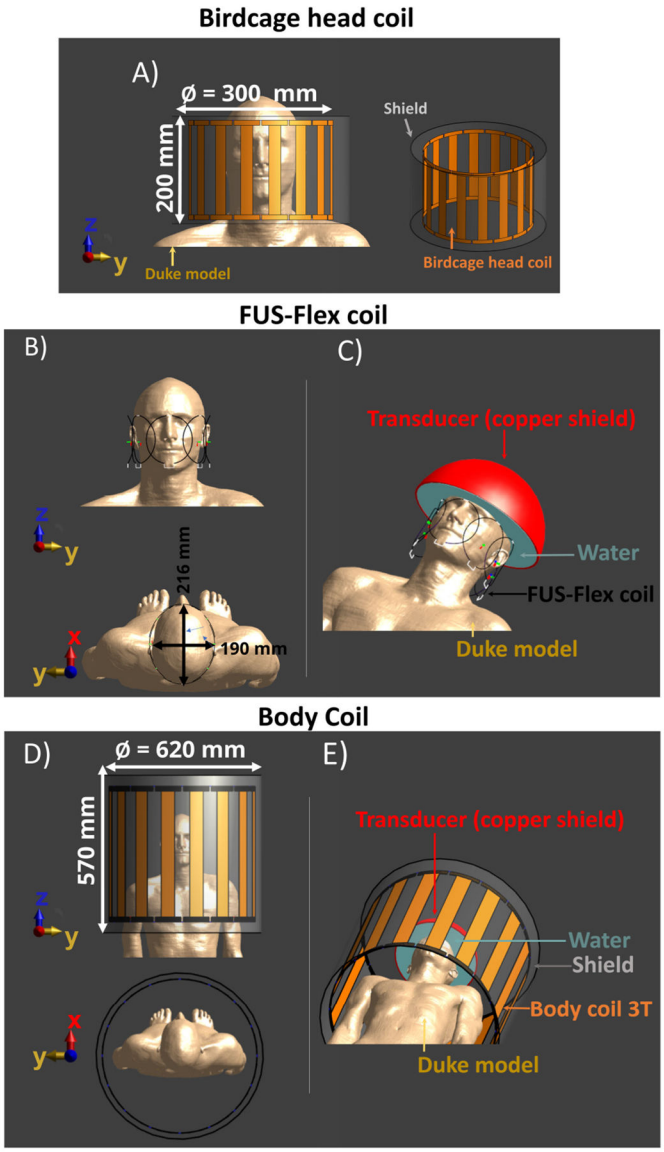

FIGURE 3.

Illustrations of the head of duke in several scenarios: A) a standard birdcage head coil geometry; B) a FUS-Flex coil, and D) a body coil geometry. The transcranial focused ultrasound transducer was modeled for use with C) a FUS-Flex coil E) a body coil geometry.

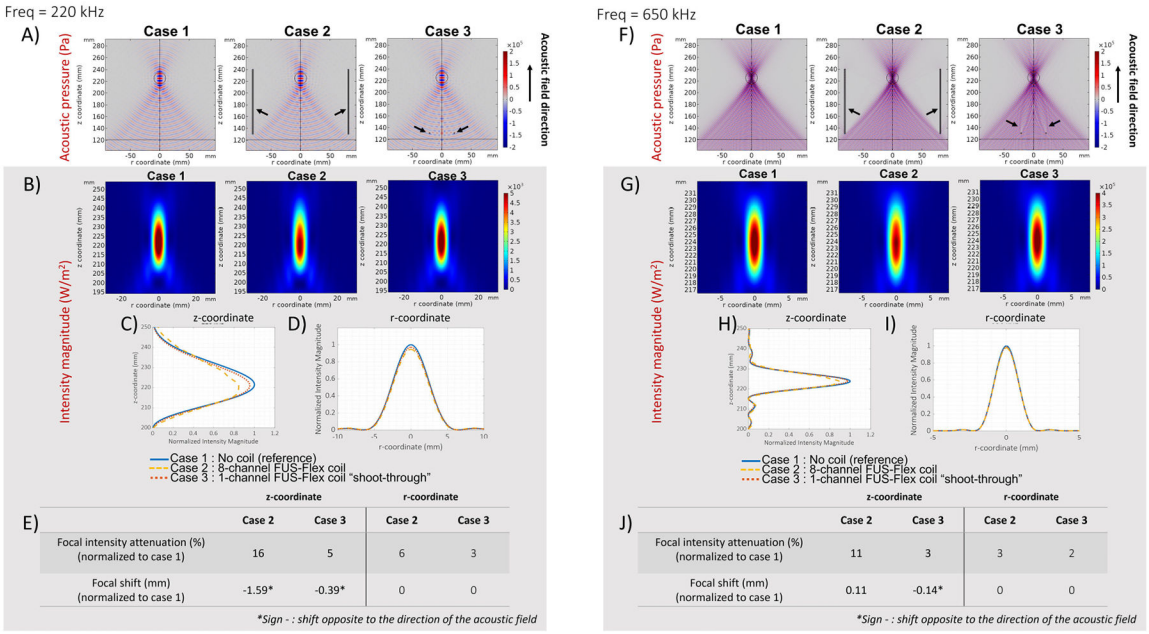

FIGURE 4.

2D map of total acoustic pressure showing the effects of the RF coil on the acoustic field:(A) 220 kHz; (F) 650 kHz. 2D map of intensity magnitude: (B) 220 kHz; (G) 650 kHz. First column: case 1 without RF coil. Second column: case 2 with coil around the focal point. Third column: case 3 FUS-Flex coil placed in the acoustic path - "shoot-through". The black arrows show the positions of the FUS-Flex coil for cases 2 and 3. Normalized radial acoustic intensity magnitude for (C, D) 220 kHz and (H, I) 650 kHz along the dotted line passing through the focal point along the *z*-coordinate. Tables showing the acoustic attenuation and the focal point shift for cases 2 and 3 normalized to the reference case without a coil (case 1) for (E) 220 kHz and (H) 650 kHz.

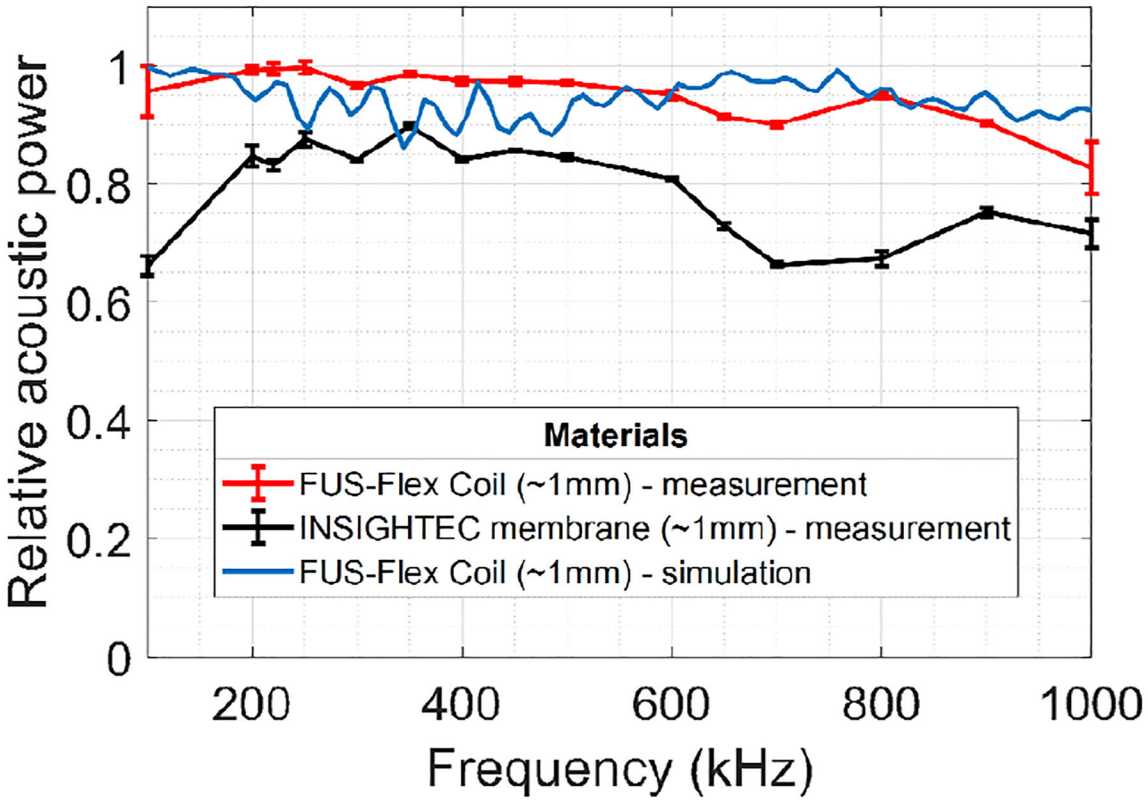

FIGURE 5.

Relative acoustic power transmitted through the FUS-Flex coil and the INSIGHTEC sealant membrane. Error bars show the standard deviation. Note that the measurement and simulated curves are not representing the exact same scenario. Measurement: single immersion transducer - simulation: 30 cm diameter focused ultrasound transducer.

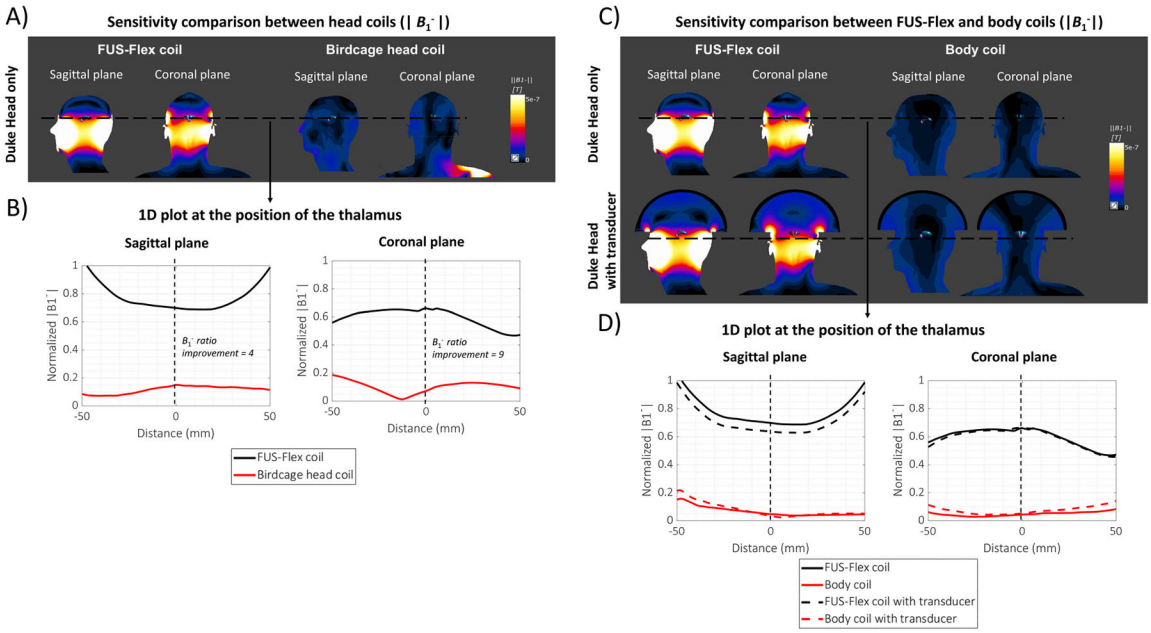

FIGURE 6.

A) Sagittal and coronal plane of the B_1^- sensitivity map for receive-only 8-channel FUS-Flex (first column) and standard birdcage head coils (second column). The origin of the simulated coordinate system is located at the center of the thalamus (blue and purple spot in the midbrain). B) 1D plot of B_1^- along the thalamus region. C) Sagittal and coronal plane of the B_1^- sensitivity map for receive-only 8-channel FUS-Flex (first column) and body coils (second column) without (first row) and with the transducer (second row). D) 1D plot of B_1^- along the thalamus region with and without the transducer.

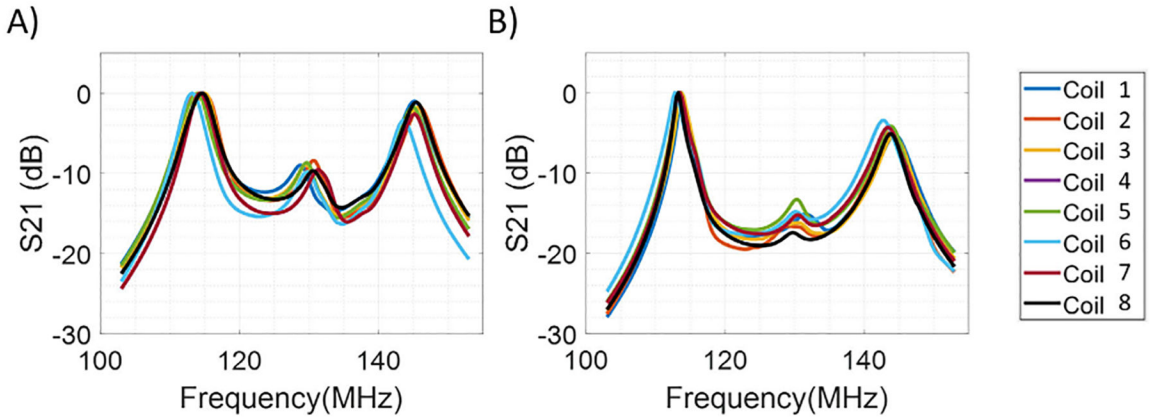

FIGURE 7.
Sensitivity measurements of each coil element separately (A) and within the array (B).

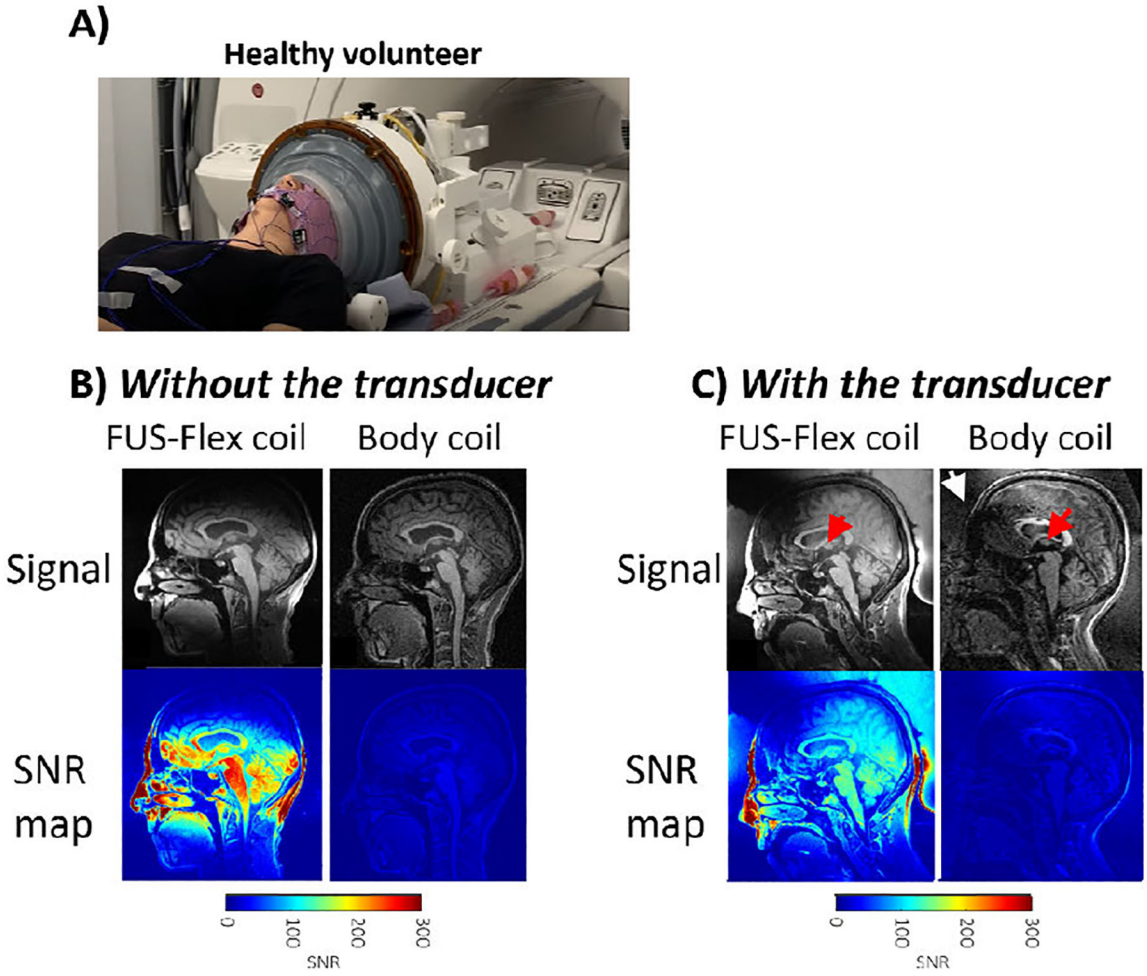

FIGURE 8.

A) Setup of the FUS-Flex coil around a healthy volunteer without the transducer. Coronal MR images and SNR maps acquired with FUS-Flex and body coils of a healthy volunteer B) in absence of the transducer and C) in presence of the transducer. In vivo images were acquired using a T1 weighted volume imaging (3D Bravo) sequence (TE = 3 ms, TR = 7.4 ms, FA = 12°, and pixel bandwidth = 244.1 Hz/px). The red and white arrows show the positions of the thalamus and the low-signal band, respectively.